

This article was downloaded by:

On: 18 January 2011

Access details: *Access Details: Free Access*

Publisher *Taylor & Francis*

Informa Ltd Registered in England and Wales Registered Number: 1072954 Registered office: Mortimer House, 37-41 Mortimer Street, London W1T 3JH, UK



International Journal of Polymeric Materials

Publication details, including instructions for authors and subscription information:

<http://www.informaworld.com/smpp/title~content=t713647664>

Hot Melt Reactive Extrusion of Chitosan with Poly(acrylic acid)

Soondeuk Jeung^a; Munmaya K. Mishra^a

^a Altria Client Services, Research, Development & Engineering, Richmond, Virginia, USA

Online publication date: 09 November 2010

To cite this Article Jeung, Soondeuk and Mishra, Munmaya K.(2011) 'Hot Melt Reactive Extrusion of Chitosan with Poly(acrylic acid)', *International Journal of Polymeric Materials*, 60: 1, 102 – 113

To link to this Article: DOI: 10.1080/00914037.2010.532524

URL: <http://dx.doi.org/10.1080/00914037.2010.532524>

PLEASE SCROLL DOWN FOR ARTICLE

Full terms and conditions of use: <http://www.informaworld.com/terms-and-conditions-of-access.pdf>

This article may be used for research, teaching and private study purposes. Any substantial or systematic reproduction, re-distribution, re-selling, loan or sub-licensing, systematic supply or distribution in any form to anyone is expressly forbidden.

The publisher does not give any warranty express or implied or make any representation that the contents will be complete or accurate or up to date. The accuracy of any instructions, formulae and drug doses should be independently verified with primary sources. The publisher shall not be liable for any loss, actions, claims, proceedings, demand or costs or damages whatsoever or howsoever caused arising directly or indirectly in connection with or arising out of the use of this material.



Hot Melt Reactive Extrusion of Chitosan with Poly(acrylic acid)

Soondeuk Jeung and Munmaya K. Mishra

Altria Client Services, Research, Development & Engineering, Richmond, Virginia, USA

The hot melt reactive extrusion of blends of chitosan and poly(acrylic acid) (PAA) was carried out without any process additives such as organic solvent or plasticizer. The maximum amount of chitosan in the blend during the extrusion process was kept at 40 wt%, since the melt viscosity of a system containing 50 wt% of chitosan exceeded the torque limitation of the equipment. The carboxylic groups of PAA interacted with the amine groups of chitosan during the melt process, and the system exhibited good melt flow. The interactions between these two polymers were explained by investigating the results obtained by thermogravimetric analysis (TGA) and differential scanning calorimetry (DSC). The thermal transition behavior of PAA was altered with a decrease of more than 10°C in the peak melting point after extrusion. The infrared (IR) spectroscopic data confirmed the existence of a complex formation and possible hydrogen bonding between chitosan and PAA during the melt process. Scanning electron microscopy (SEM) micrographs indicated that chitosan was well-dispersed in the PAA blends up to 30 wt% chitosan, with no indication of loose particles or other disruptions on the upper and lower fractured faces. This smooth interface might have been caused by the interaction between amide bonds of chitosan and carboxylic groups of PAA.

Keywords chitosan, hot melt extrusion, melt blending, poly(acrylic acid)

Received 15 September 2010; accepted 13 October 2010.

Soondeuk Jeung would like to express her appreciation for having been a past recipient of a post-doctoral fellowship awarded through the Philip Morris USA Postgraduate Research Program.

Address correspondence to Munmaya K. Mishra, Altria Client Services, Research, Development & Engineering, Richmond, Virginia, USA. E-mail: Munmaya.Mishra@altria.com

INTRODUCTION

Chitosan is of great interest in the food and pharmaceutical industries because of its biological compatibility, biodegradability, and nontoxic properties [1]. Nontoxic and environmentally friendly materials are applied in drug delivery systems, food packaging, medical sutures, and wound healing films. Chitosan and chitin are among the most common natural polymers containing glucosamine and N-acetylglucosamine repeating units in their backbone. Chitosan is obtained by N-de-acetylation from chitin, which is in turn derived from the exoskeletons of crustaceans, insects and the cell walls of microorganisms.

The applications of chitosan have been extensively reported. Gong et al. [2] reported that polyurethane-chitosan blends were prepared by a solution casting method, but the blends showed poor phase properties. Chandy et al. [3] produced biodegradable films of chitosan containing poly(ethylene glycol)(PEG) or poly(vinyl alcohol)(PVA) by the solution casting method. PEG or PVA were mixed with a solution of chitosan acetate, and was cast to a thin homogenous film with improved thermal properties. Chitosan dissolved in diluted acetic acid was added as a granulation liquid to the powder mixture [4]. After the granulation, the mass was pressed through a ram extruder and afterwards spheronized to produce pellets. Ahn et al. [5] reported a muco-adhesive polymer prepared by template polymerization of acrylic acid with chitosan. In their research, a maximum of 2.5 wt% of chitosan was dissolved in aqueous acrylic acid and the excess solvent was removed after polymerization. They found strong adhesion, limited water solubility, and an increased miscibility of poly(acrylic acid) PAA with chitosan.

The process described above involves the use of organic solvents that need to be removed afterwards, since residual solvents could induce potential hazards to the applications in the food and pharmaceutical fields. Little research has been carried out on the melt blending of chitosan with synthetic/natural polymers in the absence of solvents. Hot melt processing of a chitosan/biodegradable synthetic polymer can save energy and minimize environmental impact by minimizing waste streams needing to be further processed. The present study investigates the process of extruding chitosan without the addition of organic solvents and the production of biodegradable blends of chitosan with PAA for potential applications in the food and pharmaceutical industries. Chitosan/PAA blends were extruded using a micro-compounder and their physico-chemical properties were investigated using thermogravimetric analysis (TGA), differential scanning calorimetry (DSC), Fourier transform infrared spectroscopy (FTIR), and environmental scanning electron microscopy (ESEM).

MATERIALS AND METHODS

Materials

Chitosan was provided by Vanson Inc. and placed in a vacuum oven at 80°C for 2 h prior to use (to remove moisture). PAA (with molecular weight $M_v = 1,250,000$) was purchased from Aldrich and used as received.

Methods

Preparation of the Blends

The raw materials having the compositions of 90/10, 80/20, 70/30, 60/40 and 50/50 wt% PAA/chitosan were premixed in a mortar and a pestle (granules that needed to be broken up). The well-mixed powders were manually fed into a conical co-rotating and intermeshing micro-compounder (DACA Instruments, CA, USA). The average L/D ratio from feed to die was 5:1. Specific mechanical energy (SME) is defined as a total input of mechanical energy per unit dry weight of extrudates. The SME of various formulations during extrusion was calculated using the equation:

$$SME[\text{kJ/kg}] = \frac{2\pi\omega\tau}{1000\dot{m}}$$

Where, ω is screw speed in revolutions per minute, τ is torque in N-m and \dot{m} is mass flow rate in kg/min.

The materials had a residence time of 2 min in the micro-compounder (barrel temperature of 160°C and screw rotating speed of 100 revolutions per minute). The melt blends were extruded out from a 2 mm diameter built-in die having a rod shape. The extrudates having the compositions of 90/10, 80/20, 70/30, and 60/40 PAA/chitosan were obtained in rod-like shapes. The 50/50 PAA/chitosan blend had a distorted sheet shape since it could not flow through the die and was scraped out from the screws for the purpose of characterization.

Thermal Analysis

Thermogravimetric analysis (TGA)/differential thermal analysis (DTA) was performed with a TA Q5000 (TA Instruments). The TGA was carried out with samples of 8.0 ± 2.0 mg on a platinum pan under a nitrogen atmosphere with 5 mL/min flow rates and with a heating rate of 10°C/min to 600°C.

A modulated differential scanning calorimeter (DSC) (MDSC 2920, TA Instruments) was used to study the thermal behavior of extrudates. Extruded

pellets were ground to a fine powder in a mortar to facilitate the weighing of small amounts of the sample. Samples were carefully weighed to 9.0 ± 2.0 mg and sealed in aluminum pans with lids (hermetic pan). The temperature scan was performed from -10°C to 300°C at a heating rate of $10^{\circ}\text{C}/\text{min}$ under nitrogen atmosphere with a flow rate of $10\text{ mL}/\text{min}$.

Fourier Transform Infrared (FTIR) Analyses

FTIR spectra (wavelength with a resolution of 4 cm^{-1} and 32 scans average) were obtained using a Nexus 670, Thermo Nicolet FTIR to observe potential physical or chemical bonding between the carboxylic groups of PAA and the amine groups in chitosan. The pellets were ground and placed in a vacuum oven at 60°C for 2 h prior to testing (to remove moisture, which may interfere with the detection of hydrogen bonding) and blended with dried KBr powder and further compressed into a transparent pellet using a Thermo Nicolet die-press and placed in the FTIR spectrometer under nitrogen atmosphere. The absorbance intensity ratio (I_{1724}/I_{1074}) was determined using the FTIR software program.

Environmental Scanning Electron Microscopy (ESEM)

The morphology of hot melt blended samples was observed under environmental scanning electron microscopy (ESEM). All of the samples were fractured by mechanical bending. The broken fragments were then ground so that the opposite end of each sample was as parallel as possible to the fracture surface. The samples were then mounted vertically on 12 mm diameter carbon adhesive disks that were attached to Al stubs. The samples were sputter coated with 15 nm of Au-Pd using a Cressington 208HR sputter coater operating under argon. The samples were placed in the FEI XL30 ESEM instrument operating at 10 to 15 kV in Hi-Vac mode for imaging. The fracture surfaces were not touched during or after sample preparation.

RESULTS AND DISCUSSION

Specific Mechanical Energy (SME)

The SME was significantly influenced by the chitosan contents of the blends. The torque against the micro-extruder increased with increasing chitosan content, and the SME was proportional to the value of the torque. Torque reached a maximum value when the raw materials were fed into the micro-compounder, but after 2 min of mixing in the micro-compounder, the torque was stabilized. The resulting average SME is summarized in Table 1.

Table 1: Calculated specific mechanical energy (SME) during extrusion process.

Sample	PAA/chitosan weight composition (%)					
SME (kJ/kg)	100/0 362	90/10 482	80/20 573	70/30 681	60/40 867	50/50 8135

Thermal Analysis

Thermal degradation of chitosan/PAA was clearly demonstrated by DTA (derivative of % weight loss over temperature) shown in Figure 1. Chitosan homopolymer exhibits two distinct stages; the one at 46°C might be associated with low boiling impurities, and the other at 313°C ascribed to a complex process and maybe loss of NH₃ and other nitrogenous products, including dehydration of the saccharide rings, depolymerization, and decomposition of the acetylated and de-acetylated units of the polymer [6,7]. PAA shows four degradation steps in the differential thermogravimetric curve in Figure 1. There is no significant degradation of PAA below 200°C except for a single decomposition stage at 53°C, which might be associated with low boiling impurities from the polymer. However, the presence of a peak at 248°C in the thermogram of PAA has been reported to be associated with the dehydration and decarboxylation of polymer [1]. After the initial degradation process of PAA an intra- or inter-molecular reaction of carboxyl groups of PAA in the range of 300 and 450°C was observed. Dehydration of PAA begins above 170°C and attains a maximum rate around 250°C while decarboxylation

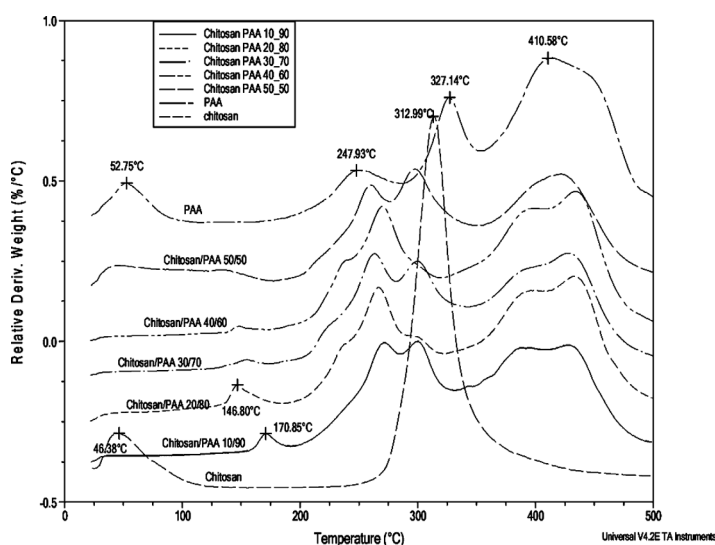


Figure 1: Differential thermogravimetric curves of PAA, chitosan homopolymers and chitosan/PAA blends.

starts at temperatures above 200°C and continues to 350°C [8]. Bulk decomposition of the polymer residue occurs at about 350°C and gives rise to highly unsaturated structures.

The thermal behavior of chitosan/PAA blends is also demonstrated in Figure 1. For the various blends three main decomposition stages were observed. The first one occurred at temperatures between 150° and 200°C depending on the composition, a mode that is absent in homopolymers. This might originate from the dehydration of the interpolymer ionic bonds and the formation of interchain amide bonds between chitosan and PAA. It has been shown that amide bond formation in chitosan-acrylic acid salts occurs above 100°C [9], and this reaction occurs when the mixture of chitosan and PAA is heated at 180°C for a certain time period. Dehydration of unreacted COOH groups of PAA in blends could also contribute to the total weight loss in the temperature range of 100–200°C in this study. The second degradation step of the blends begins at around 220°C and exhibits two stages of degradation at around 270 and 300°C. These peaks are assigned mainly to the decarboxylation of PAA at 250°C and de-acetylation of chitosan residues at around 300°C. The maximum decomposition vs. temperature in this second stage is lower than that of homopolymer, which implies instability of the polymer blends as a result of complexation during the melt process. This effect was also reported in the pyrolysis of the chitosan/carboxymethyl cellulose complex [10]. The last decomposition stage starts above 350°C and corresponds mainly to the degradation of polyacrylic chains [11].

The normalized DSC thermal scans of chitosan/PAA blends are shown in Figure 2. The thermogram of chitosan homopolymer exhibits an endothermic

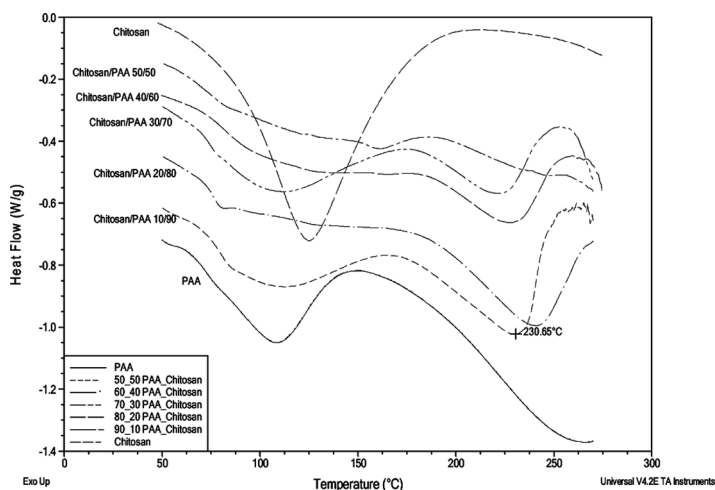


Figure 2: Differential scanning calorimetry (DSC) thermograms of chitosan, PAA homopolymers and chitosan/PAA blends.

peak at 124°C that may be associated with some sort of phase transition, even though chitosan does not have a melting point. The thermal behavior of PAA shows two endothermic peaks; one is at 108°C due to dehydration while the other is at 263°C, associated with decarboxylation. These two thermal behaviors agree with the results of thermogravimetric analysis we have reported here. The glass transition temperature (T_g) of PAA homopolymer has an onset point of 63°C, however, the T_g of chitosan/PAA is elevated by around 10°C (induced by the polymeric chain interaction associated with chitosan). The transition temperature of PAA homopolymer at 263°C was lowered to 245°C in the PAA/chitosan 90/10 blends. This indicates that the number of carboxylic acid groups in PAA is decreased by taking part in a reaction with, or hydrogen bonding to, the amine groups in chitosan.

FTIR Spectra

The FTIR study was conducted to investigate the complex formation between PAA and chitosan. The IR spectra of chitosan and PAA homopolymer

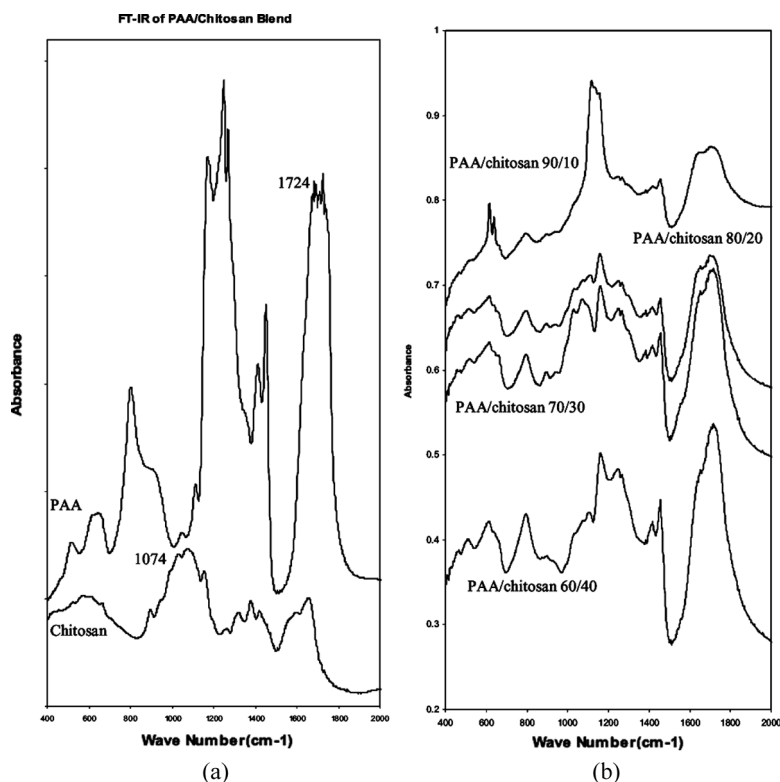


Figure 3: Infrared spectra in the region 400–2000 cm^{-1} for (a) chitosan, PAA and (b) PAA/chitosan blends.

are presented in Figure 3(a). The chitosan spectra exhibits absorption bands at 1651, 1420, 1321, 1154 and 1074 cm^{-1} assigned to amide I, $-\text{NH}_2$ bending, amide III, anti-symmetric stretching C–O–C bending and skeletal vibrations involving C–O stretching, respectively [12]. The spectra of PAA shows the absorption band at 1724 cm^{-1} due to carboxylic acid carbonyl (C=O) stretching vibration.

The IR spectra of chitosan/PAA blends prepared by the melt extrusion method are presented in Figure 3(b). The carbonyl absorption band of the PAA for the PAA/chitosan polymer blend was split into 1724 and 1708 cm^{-1} . The former is assigned to PAA homopolymer and the latter is believed to be due to the hydrogen bonding between carboxyl groups of PAA and the amino or hydroxyl groups of chitosan. This shift could happen as a result of hydrogen bonding or salt formation between chitosan and PAA during the melt process. The bands at 1423 and 1457 cm^{-1} , attributed to asymmetric and symmetric COO⁻ stretching, appear in chitosan/PAA blends together with the band at 1651 cm^{-1} due to the formation of NH_3^+ . These bands are indicative of complexation between the amino groups of chitosan and the carboxylic groups of PAA [11].

One distinct absorption band from the chitosan PAA system was selected to study the interaction between chitosan and PAA as a function of the weight fraction of chitosan in the melt blend. The ratio (I_{1724}/I_{1074}) of the intensity at 1724 cm^{-1} from PAA to 1074 cm^{-1} from chitosan was illustrated in Figure 4 as a function of the wt% of chitosan. The intensity ratio is dramatically decreased with 10 wt% chitosan to PAA; however, after 20 wt% chitosan is added to a chitosan/PAA blend, the value reaches that of chitosan homopolymer. It is interpreted that the carboxylic groups have a strong reactivity at 10 wt% addition of chitosan, and at higher concentrations the reactivity of the carboxylic groups is slightly increased.

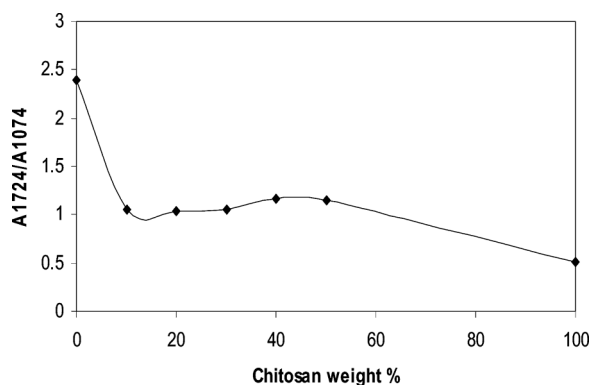


Figure 4: Composition dependence of the ratio of the intensity of the absorption band at 1724 cm^{-1} to the intensity of the absorption band at 1074 cm^{-1} .

ESEM Images and the Melt Processability of PAA/Chitosan Blends

The fracture surfaces of the PAA/chitosan polymer composite samples having the compositions 90/10, 80/20, 70/30, and 60/40 are easily extruded at 160°C resulting in a porous structure shown in Figure 5 (a) to (h). The

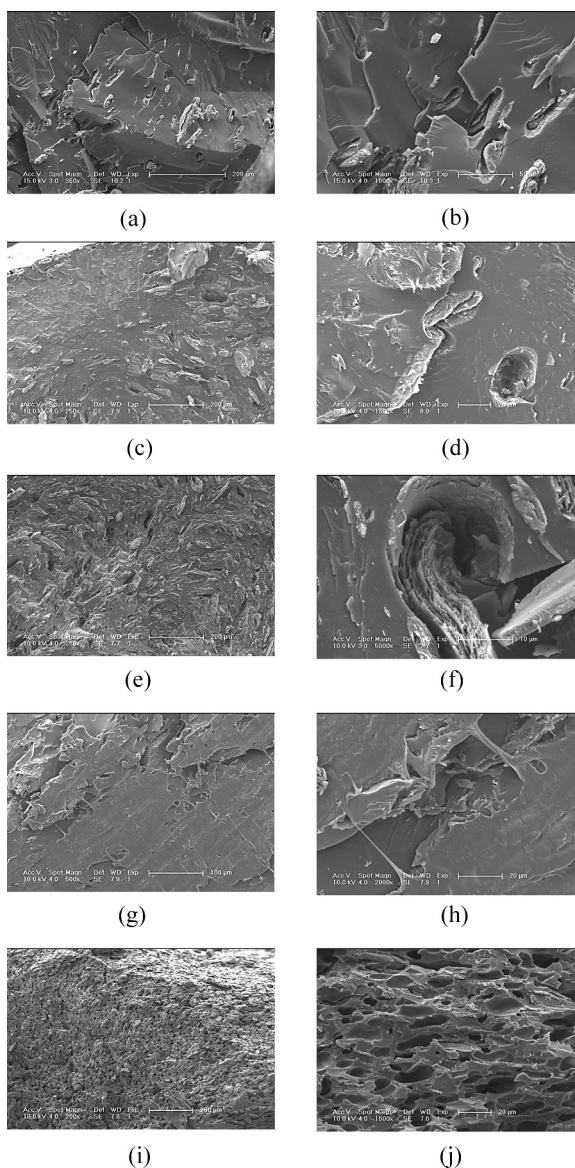


Figure 5: Scanning electron microscopy (SEM) of chitosan/PAA blends (weight %): (a)(b):10/90, (c)(d): 20/80, (e)(f): 30/70, (g)(h): 40/60, (i)(j):50/50.

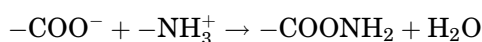
sample containing 50/50 PAA/chitosan could not be processed in the micro-compounder due to excessive viscosity. The melt blends of 50/50 PAA/chitosan were scraped directly from the twin screws and demonstrated a highly porous structure as shown in Figure 5 (i) and (j). Regardless of the composition, all of the samples' blends consisted of a solid matrix containing a random distribution of voids that were somewhat elliptical in cross-section. Some of these elliptical voids were empty; however, most of them contained material with a lamellar structure that was assumed to be particles of chitosan. These lamellae were frequently stacked and layered to mimic the shape of the elliptical void space they were present within and sometimes these lamellar structures did not appear to be in direct contact with the surrounding matrix. This was observed on the fracture surfaces of some of the samples, where individual particles constructed of layered sheets appeared to act as nucleation sites for the propagation of cracks. As the volume fraction of chitosan increased, the number of elliptical voids appeared to increase. The cross-section images indicate that the chitosan domains are 40–150 μm long with 15–30 μm thicknesses. The thickness and length of chitosan in Figure 5 is larger than that of chitosan fibers [13]. This could be induced from the agglomeration of chitosan particles during the process, giving the appearance of a sheath-like structure. The variation of the chitosan particle size might have resulted from the local variation of mechanical energy dissipation during the melt process. The upper and lower surfaces of the polymer matrix appeared smooth, with little evidence of any protrusion or loose chitosan particles in 10, 20 and 30 wt% chitosan blends.

However, when 40% chitosan was added to PAA, there was a change in the shape of the sample, and the fracture surface morphology was modified in some areas with the appearance of microfibrils extending across void spaces. This might have originated from the lack of adhesion that result in interfacial slippage between the chitosan and the polymer matrix, leading to voids and cavitations [14]. The holes resulting from the particle pull-out from the matrix is evident in most of the compositions. In addition to holes, thin wedges are also apparent in the matrix. These wedges are a result of agglomerated chitosan fibers removed from the matrix. In 40 wt% of chitosan blends, these agglomerated fibers stack up, leading to the formation of sheaths, and give rise to the cluster-like morphology of the dispersed phase. Bundles of sheaths might occur by insufficient mixing during processing.

The effect is similar to that reported for fiber-reinforced polymers. The packing density of randomly oriented fibers is low due to fiber agglomeration. When the volume fraction of fiber being compounded is greater than its natural packing density, the fibers must either break into shorter fragments or form bundles to conform to space filling requirements [15].

Adding 50% chitosan to PAA then resulted in a complete change in the shape of the sample from a rod to a distorted sheet, and the resulting

composite material was highly porous. In addition, the mechanical properties of the 50/50 PAA/chitosan polymer composite were very different from the other compositions, where the material could not be processed and fractured very easily in comparison to other samples. Phase separation between the dispersed chitosan particles and PAA is apparently observed in Figure 5 (i) and (j). The porous structure has been reported to originate from the phase separation between water and hydrated melt during processing [16]. The voids that exist in extruded samples are likely due to either the water moiety from the raw materials or water formation as a reaction by-product of carboxylic and amide group from PAA and chitosan, respectively.



The voids showed both spherical and ellipsoidal form and had a size distribution with differing sheath thickness. The number of voids increased as the concentration of chitosan increased.

CONCLUSION

Novel chitosan/PAA blends with 10/90, 20/80, 30/70 and 40/60 wt% composition were extruded without organic solvent/plasticizer. This biodegradable polymer blend could be a good potential application in food and pharmaceutical areas by reducing hazardous organic solvent and showing a good biocompatibility. Thermal behaviors of chitosan/PAA blends were investigated using thermogravimetric analysis and differential scanning calorimeter. A new degradation peak was observed between 150° and 200°C in PAA/chitosan blends in differential thermogravimetric analysis. This could be the result of interpolymeric bonds between PAA and chitosan. The glass transition and onset of melt transition temperature was also lowered more than 10°C in the PAA/chitosan melt blend compared to that of PAA homopolymers. The result of infrared spectroscopy also suggested the presence of hydrogen bonding between chitosan and PAA by the formation of a polymer complex after melt processing. FTIR analysis showed peak shifts at 1715 cm⁻¹ and 1637 cm⁻¹ as evidence of hydrogen bonding and amide linkage creation in PAA/chitosan blends. It was observed from the SEM images that chitosan particles were dispersed in the PAA polymer matrix with smooth upper and lower boundaries in 90/10, 80/20, and 70/30 PAA/chitosan blends. This smooth interface could be due to the interactions between amide bonds in chitosan and carboxylic groups in PAA. The PAA/chitosan composition at 50/50 weight %, however, showed a highly porous structure, likely due to moisture from PAA and chitosan reactions during processing.

REFERENCES

- [1] Hirano, S., Seino, H., Akiyama, Y., and Nonaka, I. (1990). *Progress in Biomedical Polymers*, Plenum, NY.
- [2] Gong, P., Zhang, L., Zhuang, L., and Lu, J. *J. Appl. Polym. Sci.* **68**, 1321 (1998).
- [3] Chandy, T., and Sharma, C. P. *J. Appl. Polym. Sci.* **44**, 2145 (1992).
- [4] Tapia, C., Buckton, G., and Newton, J. M. *Int. J. Pharm.* **92**, 211 (1993).
- [5] Ahn, J. S., Choi, H. K., and Cho, C. S. *Biomaterials* **22**, 923–928 (2001).
- [6] García, I., Peniche, C., and Nieto, J. M. *J. Thermal Anal.* **21**, 189 (1983).
- [7] Peniche-Covas, C., Argüelles-Monal, W., and San Román, J. *Polym. Deg. Stab.* **39**, 21 (1993).
- [8] Fyfe, C. A., and Kinnon, M. S. *Macromolecule.* **19**, 1909 (1986).
- [9] Qu, X., Wrzyszczyński, A., Pielichowski, K., Pielichowsky, J., Adamczak, E., Morge, S., Linden, L. A., and Rabek, J. F. *J. Macromol. Sci-Pure & Appl. Chem.* **34A**, 881 (1997).
- [10] Argüelles, Monal, W., García, I., and Peniche-Covas, C. *Polym. Bull.* **23**, 307 (1990).
- [11] Peniche, C., Argüelles, Monal W., Davidenko, N., Sastre, R., Gallardo, A., and San Román, J. *Biomaterials* **20**, 1869 (1999).
- [12] Chavasit, V., Kienzle-Sterzer, C., and Torres, J. A. *Polym. Bull.* **19**, 223 (1988).
- [13] Cartier, N., Domard, A., and Chanzy, H. *Int. J. Biol. Macromol.* **12**, 289 (1990).
- [14] Correlo, V. M., Boesel, L. F., Bhattacharya, M., Mano, J. F., Neves, N. M., and Reis, R. L., *Mater.Sci. & Eng. A* **403**, 57 (2005).
- [15] Evans, K. E., and Gibson, A. G. *Composites Sci. Tech.* **25**, 149 (1986).
- [16] Masson, J. C. (1995). *Acrylic Fiber Technology and Applications*, Marcel Dekker, New York.